Molecular Pharmacology Fast Forward. Published on August 22, 2007 as doi:10.1124/mol.107.039693

MOL 39693

Rational Engineering of Human Cytochrome P450 2B6 for Enhanced Expression and Stability: Importance of a Leu^{264}→Phe Substitution

Santosh Kumar, Yonghong Zhao, Ling Sun, Surendra S. Negi, James R. Halpert, B. K. Muralidhara

Department of Pharmacology and Toxicology (SK, LS, JRH), Department of Biochemistry and Molecular Biology (SSN), University of Texas Medical Branch, 301 University Boulevard, Galveston, TX 77555-1031

Centocor Inc., 145 King of Prussia Road, Radnor, PA 19087 (YZ)

Pfizer Inc., PhRD-Global Biologics, 700 Chesterfield Parkway West, Chesterfield, MO 63017 (BKM)

Molecular Pharmacology Fast Forward. Published on August 22, 2007 as DOI: 10.1124/mol.107.039693
This article has not been copyedited and formatted. The final version may differ from this version.

Running title: Human P450 2B6 with enhanced expression and stability

Correspondence to:

Santosh Kumar, Department of Pharmacology and Toxicology, University of Texas Medical Branch, 301 University Boulevard, Galveston, TX 77555-1031, Tel: (409) 772-9677, Fax: (409) 772-9642, Email: sakumar@utmb.edu

Number of text pages: 35

Number of Tables: 4

Number of Figures: 6

Number of References: 40

Number of words in Abstract: 248

Number of words in Introduction: 579

Number of words in Discussion: 1453

Supporting data pages: 7

Abbreviations:

P450 2B6, cytochrome P450 2B6; PCR, polymerase chain reaction; 7-EFC, 7-ethoxy-4-(trifluoromethyl)coumarin; CPR, NADPH-cytochrome P450 reductase; b_5, cytochrome b_5; H_2O_2, hydrogen peroxide; TCEP, (Tris(2-carboxyethyl)phosphine hydrochloride); CYMAL-5, 5-cyclohexylpentyl-β-D-maltoside; 4-NBP, 4-(4-nitrobenzyl)pyridine; 4-BP, 4-benzylpyridine; 4-PI, 4-phenylimidazole; 4-CPI, 4-(4-chlorophenyl)imidazole; BIF, bifonazole; BEI, 1-(2-benzyloxyethyl)imidazole; 1-BI, 1-benzylimidazole; BP, benzphetamine; GuHCl, guanidium hydrochloride; ITC, isothermal titration calorimetry.

Molecular Pharmacology Fast Forward. Published on August 22, 2007 as DOI: 10.1124/mol.107.039693
This article has not been copyedited and formatted. The final version may differ from this version.

Abstract

Despite the emerging importance of human P450 2B6 in xenobiotic metabolism, thorough biochemical and biophysical characterization has been impeded due to low expression in *Escherichia coli*. Comparison with similar N-terminal truncated and C-terminal His-tagged constructs, namely rat P450 2B1dH, rabbit 2B4dH, and dog 2B11dH, revealed that P450 2B6dH showed the lowest thermal stability, catalytic tolerance to temperature, and chemical stability against guanidium chloride-induced denaturation. Eleven P450 2B6dH mutants were rationally engineered based on sequence comparison with the three other P450 2B enzymes and the solvent accessibility of residues in the ligand-free crystal structure of P450 2B4dH. L198M, L264F, and L390P showed ~3-fold higher expression than P450 2B6dH. L264F alone showed enhanced stability against thermal and chemical denaturation compared with P450 2B6dH, and was characterized further functionally. L264F showed similar preferential inhibition by pyridine over imidazole derivatives as P450 2B6dH. The $Leu^{264}\rightarrow Phe$ substitution did not alter the K_s for inhibitors or the substrate benzphetamine, the K_m for 7-ethoxy-4-(trifluoromethyl)coumarin, or the benzphetamine metabolite profiles. The enhanced stability and monodisperse nature of L264F made it suitable for isothermal titration calorimetry studies. Interaction of 1-benzylimidazole with L264F yielded a clear binding isotherm with a distinctly different thermodynamic signature from P450 2B4dH. The inhibitor docked differently in the binding pocket of a P450 2B6 homology model than in 2B4, highlighting the different chemistry of the active site of these two enzymes. Thus, L264F is a good candidate to further explore the unique structure-function relationships of P450 2B6 using X-ray crystallography and solution thermodynamics.

Molecular Pharmacology Fast Forward. Published on August 22, 2007 as DOI: 10.1124/mol.107.039693
This article has not been copyedited and formatted. The final version may differ from this version.

For decades, cytochromes P450 from the 2B subfamily have served as a prototype for investigation of the mechanism by which P450s metabolize substrates, especially drugs and environmental contaminants, of various size, shape, and polarity. Structure-function relationships of these enzymes have been studied extensively using chimeragenesis, site-directed and random mutagenesis, molecular modeling, X-ray crystallography, and solution biophysics (Domanski and Halpert, 2001; Zhao and Halpert, 2007). X-ray structures of an engineered rabbit P450 2B4dH (N-terminal modified and C-terminal His-tag) in ligand-free (pdb:1PO5), 4-(4-chlorophenyl)imidazole **(**4-CPI)-bound (pdb:1SUO), and bifonazole (BIF)-bound (pdb:2BDM) forms have provided structural evidence that the enzyme can undergo large ligand-induced conformational changes while maintaining its overall fold (Scott et al., 2003; Scott et al., 2004; Zhao et al., 2006). Subsequently, solution thermodynamic studies using isothermal titration calorimetry (ITC) with several imidazole inhibitors of different sizes showed the flexibility of P450 2B4 in accommodating a variety of ligands (Muralidhara et al., 2006, Muralidhara and Halpert, 2007). These studies provide important insight into factors that must be considered in understanding and predicting the binding and metabolism of drugs by P450 enzymes.

Human P450 2B6 is expressed at a relatively low level in liver, comprising 1-5% of the total hepatic P450 content (Guengerich, 2005). Nonetheless, the enzyme has been found to be a primary or partial catalyst of the metabolism of an increasing number of important pharmaceuticals including cyclophosphamide, propofol, promazine, methadone, *S*-mephenytoin, efavirenz, bupropion, imipramine, midazolam, artemisinin, and tamoxifen (Rendic, 2002; Lewis et al., 2004; Zanger et al., 2007). P450 2B6 also metabolizes environmental contaminants and mutagens such as aflatoxin B_1 and styrene (Nakajima et al., 1994; Code et al., 1997). P450 2B6 is polymorphic, and more than 20 genetic variants have been identified (Lang et al., 2001;

Molecular Pharmacology Fast Forward. Published on August 22, 2007 as DOI: 10.1124/mol.107.039693
This article has not been copyedited and formatted. The final version may differ from this version.

Zanger et al., 2007). The clinical significance of these polymorphisms is emerging from a growing number of correlational analyses, in which several genetic variants of P450 2B6 were found to be linked with altered metabolism of bupropion (Kirchheiner et al., 2003), cyclophosphamide (Xie et al., 2003), and efavirenz (Ward et al., 2003). The most important mutations Q172H and K262R in variants are associated with altered enzyme activity (Lang et al., 2004; Zanger et al., 2007). The ability to predict xenobiotic metabolism and the effects of the P450 2B6 polymorphism on individual response to medications and environmental toxicants demands better understanding of structure-function relationships, especially using X-ray crystallography and solution biophysics, which has lagged behind that of other P450 2B species, such as P450 2B4. In particular, structure-function studies of P450 2B6 have been hindered by its low expression in *Escherichia coli (E. coli)* compared with other P450 2B enzymes [Scott et al., 2001]. Low expression is often accompanied by a high amount of P420 in the cell extract, leading to difficulty in purifying the P450 to homogeneity. In addition, low protein stability confounds both crystallization trials and ITC studies, which require a large amount of pure and homogenous protein samples (10-20 mg for crystallization and ITC).

Rational engineering has been effectively used to improve the stability of various proteins such as cyclophilin D (Schlatter et al., 2005**)**, the p53 core domain (Joerger et al., 2004), and mitogen-activated protein kinase p38α (Patel et al., 2004) making them amenable for robust biophysical and structural analysis. The objective of this study was to gain insight into the basis of the lower expression of P450 2B6 in order to enhance expression and stability and allow further investigation of the structure-function relationships by X-ray crystallography and solution biophysical approaches.

Molecular Pharmacology Fast Forward. Published on August 22, 2007 as DOI: 10.1124/mol.107.039693
This article has not been copyedited and formatted. The final version may differ from this version.

Materials and Methods

Materials. 7-EFC (7-ethoxy-4-(trifluoromethyl)coumarin) was purchased from Molecular Probes, Inc. (Eugene, OR). Hydrogen peroxide (H_2O_2), NADPH, tris(2-carboxyethyl)phosphine hydrochloride (TCEP), 5-cyclohexylpentyl-β-D-maltoside (CYMAL-5), guanidium hydrochloride (GuHCl), benzphetamine, and all the inhibitors: 4-CPI, BIF, 4-(4-nitrobenzyl)pyridine (4-NBP), 4-benzylpyridine (4-BP), 4-phenylimidazole (4-PI), 1-(2-benzyloxyethyl)imidazole (BEI), and 1-benzylimidazole (1-BI) were obtained from Sigma Chemical Co. (St. Louis, MO). Recombinant NADPH-cytochrome P450 reductase (CPR) and cytochrome b_5 (b_5) from rat liver were expressed in *E. coli* and prepared as described previously (Harlow and Halpert, 1997). The molecular chaperone plasmid pGro7, which expresses GroES/EL (Nakajima et al., 1994), was obtained from TAKARA BIO (Shiba, Japan). Oligonucleotide primers for polymerase chain reaction (PCR) were obtained from Sigma Genosys (Woodlands, TX). The QuikChange XL site-directed mutagenesis kit was obtained from Stratagene (La Jolla, CA). Ni-NTA affinity resin was purchased from Qiagen (Valencia, CA), and CM-Sepharose resin was purchased from Bio-Rad (Hercules, CA). All other chemicals were of the highest grade available and were obtained from standard commercial sources.

Site-directed mutagenesis. All the site-directed single mutants were created using P450 2B6dH as the template and appropriate forward and reverse primers (Table S1, Supporting Data). To confirm the desired mutation and verify the absence of unintended mutations, all constructs were sequenced in the Protein Chemistry Core Laboratory, University of Texas Medical Branch (Galveston, TX).

Expression and purification of P450 2B6dH and mutants. In general, P450 2B6dH and mutants were expressed as His-tagged proteins in *E. coli* TOPP3 and purified using a Ni-

Molecular Pharmacology Fast Forward. Published on August 22, 2007 as DOI: 10.1124/mol.107.039693
This article has not been copyedited and formatted. The final version may differ from this version.

affinity column as described previously (Scott et al., 2001). For co-expression of P450 2B6dH with chaperone, GroES/EL expressing plasmid (pGro7) and pKK2B6dH plasmid, which possessed chloramphenicol and ampicillin resistant markers, respectively, were transformed into *E. coli* JM109 cells as described recently (Mitsuda and Iwasaki, 2006). The other procedures for expression were similar to that for expression in TOPP3 cells, except that additional 25 μg/ml chloramphenicol and 2 mg/ml L-arabinose were supplemented at every step of growth. The detailed growth and P450 expression conditions in *E. coli* have been described earlier (Scott et al., 2001). To measure the expression level accurately, P450 was expressed in triplicate starting from three individual colonies in a 40 ml culture. The buffer volume in the subsequent extraction procedure was 20-25% of the culture volume as opposed to 5-10% as described earlier (Scott et al., 2001). The P450 expression in whole cell suspensions was determined by: 1) centrifuging 5 ml of the culture at 5000 g for 10 min, 2) washing the pellet in 10 ml of 0.1 M potassium phosphate (KPi), pH 7.4 and 10% glycerol, 3) re-suspending the pellet in 2.5 ml of the above buffer, and 4) measuring CO-difference spectra using 1 ml of the sample (Josephy and Logan, 2006). Because of high background the measurement of P450 expression was not sensitive at ≤100 nmol P450/liter.

P450 2B6dH and L264F for inhibitor binding and isothermal titration calorimetry (ITC) studies were extracted and purified by modifying the recently described procedure (Muralidhara et al., 2006). In brief, the cell extract was loaded onto Ni-NTA resin in the presence of detergent CYMAL-5. Protein was eluted in a high salt buffer containing 50 mM KPi (pH 7.4), 500 mM NaCl and 1 mM TECP, which facilitates subsequent binding to a CM-Sepharose column. After washing the CM-Sepharose column using low salt buffer, the protein was eluted using high salt buffer containing 10 mM KPi (pH 7.4), 500 mM NaCl, 20% glycerol, 1 mM TCEP, and 1 mM

Molecular Pharmacology Fast Forward. Published on August 22, 2007 as DOI: 10.1124/mol.107.039693
This article has not been copyedited and formatted. The final version may differ from this version.

EDTA. Protein was dialyzed twice against the above buffer without glycerol. The P450 content was measured by reduced CO-difference spectra. Protein concentrations were determined using the Bradford protein assay kit (BioRad, Hercules, CA).

Spectral studies of ligand binding. Difference spectra were recorded using 1 μM P450 on a Shimadzu 2600 spectrophotometer at 25 °C as described previously (Muralidhara et al., 2006). In brief, protein and inhibitor samples were prepared in buffer A (10 mM KPi, 500 mM NaCl, 1 mM EDTA, 1 mM TCEP, and 1 mM CYMAL-5, pH 7.4). The protein sample (3 ml) was divided into two matched quartz cuvettes, and a base line was recorded between 350 and 500 nm. Difference spectra were recorded following the addition of a series of 5-μl aliquots of inhibitor (100 μM) or benzphetamine (5 mM) to the sample cuvette and the same amount of buffer A to the reference cuvette. The spectral dissociation constants (K_s) were obtained by fitting the data to the equation for "tight binding" $2\Delta A = (\Delta A_{max} / [E_0])\ ((K_D + [I_0] + [E_0]) + ((K_D + [I_0] + [E_0]))^2 - 4[E_0][I_0])^{1/2})$ for the high affinity ligands or to the Hill equation $\Delta A = A + \Delta A_{max}[I]^n / (K_D + [I]^n)$ for the low affinity ligands using KaleidaGraph (Synergy software), as described earlier (Muralidhara et al., 2007). Benzphetamine binding data were fit to the Michaelis-Menten equation to derive the K_s value.

Enzyme assay. The standard NADPH-dependent assay for 7-EFC *O*-deethylation was essentially carried out as described (Kumar et al., 2005). Steady-state kinetic analysis of P450 2B6dH and mutants were performed at varying 7-EFC concentrations (0-150 μM). The reconstituted system contained P450 2B6dH, CPR, and b_5 at molar ratios of 1:4:2. Steady state kinetic parameters were determined by regression analysis using Sigma Plot (Jandel, San Rafel, CA). The k_{cat} and K_m values were determined using the Michaelis-Menten equation. Each

Molecular Pharmacology Fast Forward. Published on August 22, 2007 as DOI: 10.1124/mol.107.039693
This article has not been copyedited and formatted. The final version may differ from this version.

kinetic experiment included P450 2B6dH and mutants in parallel for more accurate comparison of the data.

Analysis of benzphetamine metabolites. Enzyme reconstitution and analysis of benzphetamine metabolites were done as described (Kent et.al 2004). In brief, P450 2B6dH and L264F were reconstituted separately with reductase (2 μM each) at pH 7.4. Benzphetamine was added to a concentration of 2 mM, and the reaction was initiated by the addition of 2 mM NADPH. The reaction was terminated after 30 min incubation at 30 ^{o}C by adding 8% (w/v) bicarbonate (pH 10). The metabolites were extracted with ethylacetate. The extract was acidified with a small amount of acetic acid and dried under argon. The samples were redissolved in water and analyzed by ESI-LC-MS using an Applied Biosystems 4000 QTRAP with LC Packings capillary LC system. Metabolite profiles were monitored using two independent assays and LC-MS chromatograms using appropriate standards.

Thermal stability studies. Inactivation of P450 was monitored as described previously (Kumar et al., 2006a). The reaction mixture contained 1 μM protein in 100 mM NaOH-Hepes buffer, pH 7.4. Thermal inactivation was carried out by measuring a series of absorbance spectra in the 340-700 nm range as a function of temperature between 30-70 °C with 2.5-5 °C intervals and a 3 min equilibration at each temperature. For inactivation kinetics the samples were treated at 45 °C and the spectra (340-700 nm) were recorded at different time intervals. Determination of total concentration of the heme protein was done by non-linear least square approximation of the spectra using a linear combination of spectral standards of P450 2B4 low-spin, high-spin and P420 states. All data treatment and fitting of the titration curves were performed with our SpectraLab software package (Kumar et al., 2006a). Fitting of the temperature profile and time-dependent inactivation curves was performed by regression analysis using Sigma Plot. The

Molecular Pharmacology Fast Forward. Published on August 22, 2007 as DOI: 10.1124/mol.107.039693
This article has not been copyedited and formatted. The final version may differ from this version.

inactivation profiles were fit to a two-state model to obtain the mid-point of the thermal transition temperature (T_m) (Kumar et al., 2006a), whereas a simple pseudo-first order equation was used to determine the k_{inact} values (Kumar et al., 2006b). Temperature induced protein denaturation was also followed using tryptophan at λ_{ex} = 295 nm and λ_{em} = 340 nm on a Cary Eclipse spectrofluorometer (multicell Peltier, Varian, Inc). The unfolding data points were collected at every degree between 20-90 ^{o}C with a 5 ^{o}C/min scan rate and a 12 sec equilibrium time at each temperature as described previously (Kumar et al., 2006a). A protein concentration of 5 μM was used in all the experiments, and the data were fit to a two-state transition to derive the mid-point of thermal transition ($T_{m,app}$). Since the process is irreversible, the mid-points are termed apparent.

Catalytic tolerance to temperature. The catalytic tolerance to temperature was studied by incubating enzyme (20 pmol in 20 μl dialysis buffer for two assays) at different temperatures (30-70 °C) for 10 min followed by measuring enzyme activity using a 7-EFC *O*-dethylation assay as described earlier (Kumar et al., 2006a). The temperature at which the enzyme retains 50% of the activity (T_{50}) was calculated by fitting the data to a two-state model by regression analysis using Sigma Plot.

GuHCl-induced P450 heme dissociation. P450 heme-dissociation studies were done using 5 μM protein in 50 mM KPi buffer, pH 7.4, and 2 M GuHCl in the same buffer. The proteins were incubated at various GuHCl concentrations for 1 h at 25 °C, and the spectra were recorded in the 340-700 nm range. The differential absorbance between 417 nm and 356 nm was used to calculate the extent of heme dissociation, and the data were fit to a sigmoidal equation to obtain the mid-point concentration of GuHCl ($[GuHCl]_{1/2}$) as described for P450 BioI (Lawson et al., 2004).

Molecular Pharmacology Fast Forward. Published on August 22, 2007 as DOI: 10.1124/mol.107.039693
This article has not been copyedited and formatted. The final version may differ from this version.

H_2O_2-supported P450 heme depletion. Determination of the kinetics of P450 2B6dH heme depletion in the presence of H_2O_2 was conducted under conditions similar to those previously described for P450 2B1dH (Kumar et al., 2006a). The reaction was carried out at 25 °C in 100 mM NaOH-Hepes buffer, pH 7.4, in 1-ml semi-micro spectrophotometric cell with constant stirring using a Shimadzu-2600 spectrophotometer. The reaction mixture contained 1 μM protein and 60 mM H_2O_2. Bleaching of the hemoprotein was followed by measuring a series of absorbance spectra in the 340-700 nm range. Each series contained at least 10 spectra. Determination of the total concentration of the heme protein and data fitting to determine the k_{inact} values were done as described above.

ITC experiments of 1-BI binding to P450 2B6dH L264F. ITC experiments were performed on a VP-ITC instrument interfaced with a computer for data acquisition and analysis using Origin Version 7 software (MicroCal LLC, Northampton, MA), as described previously (Muralidhara et al., 2006). In brief, protein and ligand samples were pre-incubated to the required temperature using a ThermoVac (Microcal LLC.) and loaded into the calorimeter cell and titration syringe, respectively. ITC experiments were done using 50 mM KPi buffer, pH 7.4, containing 500 mM NaCl, 1 mM EDTA, 1 mM TCEP, and 1 mM CYMAL-5. A typical titration schedule included addition of 5 μl per injection of 1-BI with 25 injections spaced at 5 min intervals. The titration cell was continuously stirred at 300 rpm. For the first injection only, 2 μl of ligand was added and the corresponding data point was deleted from the analysis. The binding isotherms were best-fit to a one-set binding-site model by Marquardt non-linear least-square analysis to obtain binding stoichiometry (N), association constant (K_a) and thermodynamic parameters of interaction using Origin 7.0 software (Microcal LLC).

Molecular Pharmacology Fast Forward. Published on August 22, 2007 as DOI: 10.1124/mol.107.039693
This article has not been copyedited and formatted. The final version may differ from this version.

Results

Coexpression of 2B6dH with the chaperone GroEL/ES and purification: The low expression of P450 2B6dH (50-75 nmol/liter) as a result of rapid inactivation into P420 made it very difficult to purify the enzyme to homogeneity for biochemical and biophysical characterization (Scott et al., 2001). Therefore, effort was made to enhance the expression by co-expressing P450 2B6dH with the molecular chaperones GroEL/ES, which yielded a >3-fold enhanced expression. The enzyme was successfully purified to >95% enrichment using a modified purification procedure as described in Materials and Methods. The purified P450 2B6dH had: 1) a specific content of ~ 18 nmol of P450 per mg protein, 2) a ratio of Soret absorbance to the protein band at 280 nm (A_{418}/A_{280}) of 1.6 (Fig. 1A), and 3) a reduced-CO difference spectral maximum at 449 nm with a minimal shoulder around 420 nm (Fig. 1B). However, the above modification did not yield P450 2B6dH in large quantity or a sufficiently homogeneous state for X-ray crystallography or ITC studies. Therefore, the purified P450 2B6dH was further studied to investigate the basis of low expression and rapid inactivation into P420 in order to enhance the expression and stability.

Stability of P450 2B enzymes. Low P450 expression and high P420 content are usually associated with low thermal stability. Therefore, P450 2B1dH, 2B4dH, 2B6dH, and 2B11dH were studied for thermal stability, catalytic tolerance to temperature, and susceptibility to GuHCl induced denaturation, as described in Materials and Methods. The results presented in Table 1 (see also Fig. S1 of Supporting Data) show that P450 2B1dH is the most thermally stable enzyme followed by P450 2B4dH. P450 2B6dH displayed the lowest thermal stability. The T_m for P450 2B6dH was ~13 ^oC lower than the T_m of P450 2B1dH. P450 2B11dH also showed a 10 ^oC lower T_m than P450 2B1dH. In the temperature-dependent protein denaturation monitored by

Molecular Pharmacology Fast Forward. Published on August 22, 2007 as DOI: 10.1124/mol.107.039693
This article has not been copyedited and formatted. The final version may differ from this version.

Trp fluorescence (Fig S1 of Supporting Data) P450 2B6dH showed a $T_{m,app}$ of ~3 ^{o}C less than P450 2B1dH (Table 1). P450 2B1dH showed the highest catalytic tolerance to temperature followed by P450 2B4dH (Table 1) (see also Fig. S2 of Supporting Data). The T_{50} of P450 2B6dH was 7.5 ^{o}C lower than the T_{50} of P450 2B1dH. The heme-dissociation assay exhibited 3-fold lower $[GuHCl]_{1/2}$ for P450 2B6dH compared with P450 2B1dH (0.41 vs. 1.20 M), suggesting that P450 2B6dH is also less stable against chemical denaturation. Although the relative P450 stability and expression did not correlate well in the case of P450 2B11dH, the data suggested that to some extent the lower thermal stability of P450 2B6dH results in lower expression.

Rational engineering of P450 2B6dH for enhanced expression and stability. The marked differences in expression levels and thermal stability of the P450 2B enzymes provide immediate leads for identification of residues that may be associated with the lower expression and stability of P450 2B6dH. P450 2B1dH, 2B4dH, 2B6dH, and 2B11dH share greater than 75% sequence identity. Residues at 25 positions (58, 82, 103, 119, 129, 130, 154, 193, 197, 198, 212, 213, 214, 262, 264, 271, 284, 326, 341, 350, 354, 373, 374, 390, and 394) are identical in P450 2B1dH, 2B4dH, and 2B11dH, but different in P450 2B6dH. These residues were mapped onto the ligand-free structure of P450 2B4dH, and the solvent accessible surface area of each residue was calculated using the GETAREA program (Fraczkiewicz and Braun, 1998). Residues at positions 58, 103, 129, 154, 198, 264, 284, 350, 354, 390, 394 were classified as buried based on the low solvent accessible surface area and are shown on a homology model of P450 2B6dH (Fig. 2.) On the hypothesis that some of these residues are associated with low stability and/or impaired folding of P450 2B6dH leading to low expression, we replaced each residue with the

Molecular Pharmacology Fast Forward. Published on August 22, 2007 as DOI: 10.1124/mol.107.039693
This article has not been copyedited and formatted. The final version may differ from this version.

corresponding residue in 2B1dH, 2B4dH, or 2B11dH to create F58L, M103V, V129L, I154V, M198L, L264F, S284H, E350D, Y354H, L390P, and T394S.

Expression and purification of engineered P450 2B6dH mutants. The mutants were first expressed in TOPP3 cells in a 40 ml culture, and P450 was extracted as described in Materials and Methods (Table 2). M198L, L264F, and L390P showed a >3-fold higher expression than P450 2B6dH in cell extracts. These mutants as well as Y354H also showed higher expression than P450 2B6dH when P450 was measured in whole cell suspension (Table 2). Therefore, M198L, L264F, Y354H, and L390P were expressed in the presence of the chaperone GroEL/ES, and P450 was measured in cell extracts. M198L and L264F showed ~2-fold higher expression, while L390P showed a >3-fold higher expression than P450 2B6dH. Furthermore, large-scale expression (>1 liter) in the presence of chaperone and efficient extraction procedures yielded up to 400 nmol/liter of P450 2B6dH and 1000 mmol/liter of M198L, L264F, and L390P (data not shown). M198L and L390P showed a specific content of ~17 nmol/mg protein and ~10% P420 content, whereas L264F showed a specific content of 20 nmol of P450/mg protein and <1% P420 content.

Steady-state kinetic analysis with 7-EFC. Steady-state kinetic analysis of 7-EFC *O*-deethylation by M198L, L264F, and L390P yielded k_{cat} values of 1.8, 2.0, and 1.7/min, respectively, compared with 3.0/min of P450 2B6dH. The K_m values of M198L, L264F, and L390P were unaltered compared with P450 2B6dH (36.6, 36.1, and 32.3 vs. 30.4 μM).

Stability of P450 2B6dH mutants. M198L, L264F, and L390P were studied for structural and catalytic stability and the results are presented in Fig. 3 and Table 3. L264F showed ~4 ^{o}C higher, whereas M198L and L390P showed 2 and 4 ^{o}C lower T_m than P450 2B6dH, respectively (Fig. 3A, Table 3). Subsequently, the inactivation rate constant of P450

Molecular Pharmacology Fast Forward. Published on August 22, 2007 as DOI: 10.1124/mol.107.039693
This article has not been copyedited and formatted. The final version may differ from this version.

2B6dH, M198L, L264F, and L390P was determined at 45 ^{o}C (Fig. 3B). The k_{inact} for L264F was ~3-fold lower, but for M198L and L390P 5-fold higher than P450 2B6dH (Table 3). Similarly, L264F displayed a 1.5 ^{o}C higher $T_{m,app}$ than P450 2B6dH (Table 3), further suggesting that L264F is the most thermally stable P450 2B6dH.

Catalytic tolerance to temperature was also determined for P450 2B6dH and the mutants. L264F showed ~1 ^{o}C higher, whereas M198L and L390P showed >3 ^{o}C lower T_{50} than P450 2B6dH (Table 3 and Fig. S3, Supporting Data). These results suggest that the improvement in thermal stability of L264F is perhaps because of a decrease in P450 unfolding rather than a decrease in heme removal. Therefore, H_2O_2- and GuHCl-induced heme-dissociation assays were carried out. L264F showed a negligible decrease, whereas M198L and L390P showed a ~2-fold increase in k_{inact} by H_2O_2 compared with P450 2B6dH (Table 3 and Fig. S4, Supporting Data). Similarly, L264F exhibited a modest increase, whereas L390P showed a modest decrease in $[GuHCl]_{1/2}$ compared with P450 2B6dH (Table 3and Fig. S5, Supporting Data).

Unaltered functional properties of L264F. The spectral dissociation constants (K_s) of selected imidazole and pyridine derivatives and benzphetamine binding to P450 2B6dH and L264F were determined (Table 4). Most imidazole and pyridine derivatives induced type II difference spectra with a peak around 430 nm and a trough around 400 nm (data not shown). For the pyridine derivatives, the K_s values varied from 0.07 μM for 4-NBP to 0.53 μM for 4-BP. Similarly, for the imidazole derivatives K_s varied from 0.1 μM for 4-PI to 2 μM for 1-BI. Both P450 2B6dH and L264F showed typical type-I spectra of benzphetamine binding with K_s values of 53 and 61 μM, respectively. Representative spectra of benzphetamine (Fig. 4B) and 4-CPI (Fig. 4A) binding are shown. The very similar spectral binding constants with various inhibitors and benzphetamine suggested that the Leu^{264}→Phe substitution does not perturb the active site.

Molecular Pharmacology Fast Forward. Published on August 22, 2007 as DOI: 10.1124/mol.107.039693
This article has not been copyedited and formatted. The final version may differ from this version.

Benzphetamine metabolite profiles were also assayed to study the active site integrity of L264F. As shown in Fig 4C, the metabolite profiles of 2B6dH and L264F were identical, consisting of norbenzphetamine (226.2) as a major and OH-norbenzphetamine (242.2) and OH-benzphatamine (256.2) as minor metabolites.

Thermodynamics of 1-BI binding to L264F. The binding of 1-BI to L264F was further investigated by ITC to obtain thermodynamic parameters. Ultracentrifugation experiments showed that P450 2B6dH exists as a mixture of dimer and higher order oligomers (data not shown). However, L264F exists as a clear dimer and remains dimeric upon 1-BI binding, which allows a clean interpretation of calorimetric binding data. Binding of 1-BI induced an unusual spectrum (Fig 5, *inset a*) with no evidence of N-coordination to the heme iron. In ITC, a good binding isotherm was obtained for 1-BI binding to L264F as shown in Fig. 5. Binding of 1-BI to L264F was an entropically driven process with ΔG = -7.2 kcal/mol, ΔH = 2.1 kcal/mol, $-T\Delta S$ = 9.2 kcal/mol, and a 1:1 stoichiometry. In contrast, binding of 1-BI to P450 2B4dH was an enthalpically driven and exothermic process, with typical a type-II spectrum and a spectral dissociation constant of 0.06 μM (Muralidhara et at., 2006).

Molecular Pharmacology Fast Forward. Published on August 22, 2007 as DOI: 10.1124/mol.107.039693
This article has not been copyedited and formatted. The final version may differ from this version.

Discussion

The discovery of an increasing number of drugs that are metabolized by P450 2B6 and of numerous polymorphic variants with altered function and/or expression has greatly enhanced the interest in elucidating its structure-function relationships (Zanger et al., 2007). However, low expression in *E. coli*, perhaps as the result of low stability, causes difficulty in purifying P450 2B6 to homogeneity and in high yield, thus impeding thorough biochemical and biophysical characterization (Scott et al., 2001). In this study we systematically investigated the expression and stability of P450 2B6dH and then utilized a rational approach to engineered the enzyme for enhanced expression and/or stability. Among eleven site-directed mutants M198L, L264F, and L390 showed >3-fold higher expression than P450 2B6dH, and L264F displayed a ~4 ^{o}C higher T_m and ~3-fold lower k_{inact} by temperature than P450 2B6dH. The Leu^{264}→Phe substitution does not alter significantly the binding affinity with selected pyridine and imidazole inhibitors or benzphetamine, enzyme activity with 7-EFC, or metabolite profiles with benzphetamine. The mutant also withstands robust stirring conditions and long experimental time scales (~2 h at 25 ^{o}C), thus making it possible to obtain a clear ITC binding isotherm with 1-BI. Therefore, L264F should be suitable for further structure-functional studies using, but not limited to, ITC and X-ray crystallography.

A large number of comparative structural and mutagenesis studies on other proteins have revealed some general strategies for increasing protein stability. These include: increasing the hydrophobic packing in the interior, extending networks of salt-bridges and hydrogen bonds, increasing the extent of secondary structure formation, shortening or strengthening solvent-exposed loops and termini, and replacing residues responsible for irreversible chemical alterations of the protein structure (Eijsink et al., 2004). Each of these general rules may or may

Molecular Pharmacology Fast Forward. Published on August 22, 2007 as DOI: 10.1124/mol.107.039693
This article has not been copyedited and formatted. The final version may differ from this version.

not be applied successfully to a given protein. For example, mutagenesis studies and crystal structures showed that two aromatic clusters are important for the thermal stability of the thermophilic P450 119 from *Sulfolobus solfataricus* (Nishida et al., 2005). However, the crystal structure of P450 175A1 shows that aromatic clusters are not present in this thermophilic P450, suggesting that its thermal stability is achieved through other mechanisms (Yano et al., 2003). Relatively little is known about the structural determinants of mammalian P450 stability. An empirical approach to improve protein stability based on comparison of sequences of homologous proteins has been employed in proteins such as the DNA binding domain of human p53 (Nikolova et al., 1998), phytase (Lehmann et al., 2002), and 3-isopropylmalate dehydrogenase (Watanabe et al., 2006). The difference in expression levels and thermal stability of orthologous P450 2B enzymes provided an immediate lead for identification of residues that might be associated with the low expression and/or stability of P450 2B6dH (Table 1). The residues identified (198, 264, 390) are outside of the active site, and the mechanism by which mutations enhance expression or stability is unclear. Prior work has shown that a $Met^{198}\rightarrow$Thr substitution as in the P450 2B6*27 variant caused decreased enzyme activity (Rotger et al., 2007). It can be speculated that the $Leu^{264}\rightarrow$Phe substitution increases the hydrophobicity or integrity of the H-helix, which in turn makes the protein more robust. Phe-264 is the first residue in helix H in the 2B4 structure (Scott et al., 2003).

Comparison of the wild-type and mutant 2B enzymes showed a discordance between expression levels and stability. Thus, although M198L and L390P in P450 2B6dH showed enhanced expression, thermal stability was decreased. Furthermore, although P450 2B11dH showed much higher expression than P450 2B6dH (Scott et al., 2001), thermal stability of P450 2B11dH was only slightly higher than P450 2B6dH (Table 1). In contrast, P450 2B1dH and

Molecular Pharmacology Fast Forward. Published on August 22, 2007 as DOI: 10.1124/mol.107.039693
This article has not been copyedited and formatted. The final version may differ from this version.

2B4dH showed higher expression (Scott et al., 2001) as well as thermal stability than P450 2B6dH (Table 1). It is interesting to note that the protein thermal stability decreases in the order: rat 2B1 > rabbit 2B4 >> dog 2B11 ≥ human 2B6, which may be correlated with the time-line of the evolution of these enzymes/mammals. Xenobiotic-metabolizing human 2B6, which appears to have evolved last among the 2B enzymes (Thomas, 2007), is the least stable. The results with various P450 2B enzymes (Table 1) and 2B6dH and its mutants (Table 3) clearly suggest that there is only a subtle difference in the protein structural stability ($T_{m,app}$). However, large differences among the enzymes can be seen in properties that are directly related to the heme (T_m, activity, and H_2O_2- and GuHCl-dependent heme dissociation). It is possible that M198L and L390P achieve higher expression by incorporating heme effectively and forming relatively lower amounts of apo-protein. Decreased thermal stability of M198L and L390P could also account for rapid formation of P420 and/or apo-protein compared with P450 2B6dH and L264F. In addition, a higher rate of P450 inactivation by heme depletion was observed in M198L and L390P than L264F. Comparison of the relative expression, thermal stability, and the amount of P420 in the P450 2B enzyme samples, suggests that the lower expression and thermal stability of P450 2B6dH may reflect a higher rate of P450 degradation into P420 and heme dissociation.

In contrast, L264F showed enhanced expression as well as increased thermal stability compared with P450 2B6dH. Thus the Leu^{264}→Phe substitution may lead to increased incorporation of heme and decreased P450 degradation into P420 or apo-protein, as deduced from the fact that the purified L264F had a negligible amount of P420, whereas P450 2B6dH, M198L, and L390P had 8-10% P420. Clearly, thermal and H_2O_2-supported inactivation of P450 indicates that the Leu^{264}→Phe substitution slows down the rate of protein unfolding without increasing the accessibility of the heme, suggesting that this substitution stabilizes the surface

Molecular Pharmacology Fast Forward. Published on August 22, 2007 as DOI: 10.1124/mol.107.039693
This article has not been copyedited and formatted. The final version may differ from this version.

domain (consistent with a subtle increase of $T_{m,app}$ by 1.5 ^{o}C). An unaltered rate of heme depletion in L264F compared with P450 2B6dH is also consistent with largely unaffected catalytic tolerance to temperature. Because only one of the eleven mutants showed enhanced stability as well as expression compared with the wild-type, the "rational" approach employed here appears to have limitations. Therefore, alternate rational approaches are needed to enhance the stability of the important human P450 2B6. One such approach could be identification of the residues that are identical in the more stable P450 2B1dH and 2B4dH (set 1) and identical in the less stable 2B6dH and 2B11dH (set 2) but where the residue in set 1 is different from the residue in set 2.

P450 2B6dH and L264F showed indistinguishable spectral binding properties with inhibitors, including preference for pyridine over imidazole derivatives (Table 4), whereas the opposite was true in the case of P450 2B4dH (Scott et al., 2004; Muralidhara et al., 2006; data not shown). In particular, 1-BI binds ~45-fold less tightly to P450 2B6dH than P450 2B4dH, and the difference spectrum indicates the lack of N-coordination of 1-BI to the 2B6dH heme iron, as opposed to the typical type-II spectrum in the case of P450 2B4dH. Therefore, 1-BI and 4-CPI (positive control) were docked in the active site of P450 2B6 model (Fig. 6). While 4-CPI docked perfectly as one low energy (6.52 kcal/mol) ensemble similar to the one seen in the 2B4 crystal structure (Zhao et al., 2006), 1-BI docked in multiple orientations, including the imidazole nitrogen-coordination with the heme. In the figure we have shown the 1-BI docking as a low energy (6.17 kcal/mol) conformation, which is consistent with our solution findings that 1-BI induced a weak and non-type II spectrum. In this conformation the benzene ring lies parallel to the heme (red) plane, and the imidazole nitrogen is pointed away from the heme iron in 1-BI structure. Although the detailed structural explanation for this observation is

Molecular Pharmacology Fast Forward. Published on August 22, 2007 as DOI: 10.1124/mol.107.039693
This article has not been copyedited and formatted. The final version may differ from this version.

inconclusive, one can clearly see a big kink in the middle of helix I, which could potentially put steric constraints on the binding pocket on top of the heme plane. Between P450 2B4dH and 2B6dH only two putative active site residues 103 and 363 are distinct. Therefore, it is highly likely that residues outside of the active site may contribute the differences in the relative binding affinity between the two enzymes. In addition to the spectral and computational findings, the increased stability of P450 2B6dH L264F allowed ITC studies of 1-BI binding that were not possible with 2B6dH itself, which revealed a very different thermodynamic signature compared with binding to P450 2B4dH (Muralidhara et al., 2006). Specifically, the weaker binding of 1-BI to 2B6dH L264F is entropically-driven, as opposed to the stronger, enthalpically-driven binding to P450 2B4dH. Clearly, highly expressed, stable, and homogenous L264F should prove an invaluable template for further study using biochemical and biophysical methods, especially X-ray crystallography and ITC. Questions of interest include the differences in inhibitor sensitivity compared with P450 2B4 and the structural basis of alterations in P450 2B6 function resulting from single nucleotide polymorphisms outside of the active site.

Molecular Pharmacology Fast Forward. Published on August 22, 2007 as DOI: 10.1124/mol.107.039693
This article has not been copyedited and formatted. The final version may differ from this version.

References

Code EL, Crespi CL, Penman BW, Gonzalez FJ, Chang TK and Waxman DJ (1997) Human cytochrome P4502B6: interindividual hepatic expression, substrate specificity, and role in procarcinogen activation. *Drug Metab Dispos* **25**:985-993.

DeLano, WL (2004) *The PyMol User's Manual*, DeLano Scientific LLC, San Carlos, CA.

Domanski TL and Halpert JR (2001) Analysis of mammalian cytochrome P450 structure and function by site-directed mutagenesis. *Curr Drug Metab* **2**:117-137.

Eijsink VG, Bjork A, Gaseidnes S, Sirevag R, Synstad B, van den Burg B and Vriend G (2004) Rational engineering of enzyme stability. *J Biotechnol* **113**:105-120.

Fraczkiewicz R and Braun W (1998) Exact and efficient analytical calculation of the accessible surface area and their gradient for macromolecules. *J Comput Chem* **19**:319-333.

Guengerich FP (2005) Human cytochrome P450 enzymes. *Cytochrome P450: structure, mechanism, and biochemistry* 3rd ed., P. R. Ortiz de Montellano (ed.), Plenum Press, New York. p. 377-530.

Harlow GR and Halpert JR (1997) Alanine-scanning mutagenesis of putative substrate recognition sites in human cytochrome P4503A4. *J Biol Chem* **272**:5396-5402

Joerger AC, Allen MD and Fersht AR (2004) Crystal structure of a superstable mutant of human p53 core domain: insights into the mechanism of rescuing oncogenic mutations. *J Biol Chem* **279**:1291-1296.

Josephy D and Logan D (2007) whole cell assay for spectroscopic measurement of recombinant cytochrome P450 expression in bacteria. *Varian* http://www.varianinc.com/cgi-bin/nav?applications/apps/uv86&cid=HFIH.

Molecular Pharmacology Fast Forward. Published on August 22, 2007 as DOI: 10.1124/mol.107.039693
This article has not been copyedited and formatted. The final version may differ from this version.

Kent UM, Pascual L, Roof RA, Ballou DP and Hollenberg, PF (2004) Mechanistic studies with N-benzyl-1-aminobenzotriazole-inactivated CYP2B1: Differential effects on the metabolism of 7-ethoxy-4-(trifluoromethyl)coumarin, testosterone, and benzphetamine. *Arch Biochem Biophys* **423**:277-287.

Kirchheiner J, Klein C, Meineke I, Sasse J, Zanger UM, Murdter TE, Roots I and Brockmoller J (2003) Bupropion and 4-OH-bupropion pharmacokinetics in relation to genetic polymorphisms in CYP2B6. *Pharmacogenetics* **13**:619-626.

Lawson RJ, Leys D, Sutcliffe MJ, Kemp CA, Cheesman MR, Smith SJ, Clarkson J, Smith WE, Haq I, Perkins JB and Munro AW (2004) Thermodynamic and biophysical characterization of cytochrome P450 BioI from Bacillus subtilis. *Biochemistry* **43**:12410-12426.

Kumar S, Chen CS, Waxman DJ and Halpert JR (2005) Directed evolution of mammalian cytochrome P450 2B1: mutations outside of the active site enhance the metabolism of several substrates, including the anticancer prodrugs cyclophosphamide and ifosfamide. *J Biol Chem* **280:**19569-19575.

Kumar S, Sun L, Liu H, Muralidhara BK and Halpert JR (2006a) Engineering mammalian cytochrome P450 2B1 by directed evolution for enhanced catalytic tolerance to temperature and dimethyl sulfoxide. *Protein Eng Des Select* **34**:1958-1965.

Kumar S, Liu H and Halpert JR (2006b) Engineering of cytochrome P450 3A4 for enhanced peroxide-mediated substrate oxidation using directed evolution and site-directed mutagenesis. *Drug Metab Dispos* **19**:547-554.

Lang T, Klein K, Fischer J, Nussler AK, Neuhaus P, Hofmann U, Eichelbaum M, Schwab M and Zanger UM (2001) Extensive genetic polymorphism in the human CYP2B6 gene with impact on expression and function in human liver. *Pharmacogenetics* **11**:399-415.

Lehmann M, Loch C, Middendorf A, Studer D, Lassen SF, Pasamontes L, van Loon AP and Wyss M (2002) The consensus concept for thermostability engineering of proteins: further proof of concept. *Protein Eng* **15**:403-411.

Lewis DF, Lake BG and Dickins M (2004) Substrates of human cytochromes P450 from families CYP1 and CYP2: analysis of enzyme selectivity and metabolism. *Drug Metabol Drug Interact* **20:**111-142.

Mitsuda M and Iwasaki M (2006) Improvement in the expression of CYP2B6 by co-expression with molecular chaperones GroES/EL in *E. coli*. *Protein Expr Purif* **46**:401-405.

Muralidhara BK, Negi S, Chin CC, Braun W and Halpert JR (2006) Conformational flexibility of mammalian cytochrome P4502B4 in binding imidazole inhibitors with different ring chemistry and side chains - Solution thermodynamics and molecular modeling. *J Biol Chem* **281**:8051-8061.

Muralidhara BK, Negi S and Halpert JR (2007) Dissecting the thermodynamics and cooperativity of ligand binding in cytochrome P450eryF. *J Am Chem Soc*. **129**: 2015-2024.

Muralidhara BK and Halpert, JR (2007) Thermodynamics of ligand binding to P450 2B4 and P450eryF studied by isothermal titration calorimetry. *Drug Metab Rev* In Press

Nakajima T, Elovaara E, Gonzalez FJ, Gelboin HV, Raunio H, Pelkonen O, Vainio H and Aoyama T (1994) Styrene metabolism by cDNA-expressed human hepatic and pulmonary cytochromes P450. *Chem Res Toxicol* **7**:891-896.

Nikolova PV, Henckel J, Lane DP and Fersht AR (1998) Semirational design of active tumor suppressor p53 DNA binding domain with enhanced stability. *Proc Natl Acad Sci* USA **95**:14675-14680.

Nishida CR and Ortiz de Montellano PR (2005) Thermophilic cytochrome P450 enzymes. *Biochem Biophys Res Commun* **338**:437-445.

Patel SB, Cameron PM, Frantz-Wattley B, O'Neill E, Becker JW and Scapin G (2004) Lattice stabilization and enhanced diffraction in human p38 alpha crystals by protein engineering. *Biochim Biophys Acta* **1696**:67-73.

Rendic S (2002) Summary of information on human CYP enzymes: human P450 metabolism data. *Drug Metab Rev* **34**:83-448.

Rotger M, Tegude H, Colombo S, Cavassini M Furrer H, De´costerd L, Blievernicht J, Saussele T, Günthard HF, Schwab M, Eichelbaum M, Telenti A and Zanger UM (2007) Predictive Value of Known and Novel Allelesof CYP2B6 for Efavirenz Plasma Concentrations in HIV-infected Individuals. *Cli Pharmacol Therap* E. Pub. 18 Jan 2007. DOI:10.1038/sj.clpt.6100072.

Schlatter D, Thoma R, Kung E, Stihle M, Muller F, Borroni E, Cesura A and Hennig M (2005) Crystal engineering yields crystals of cyclophilin D diffracting to 1.7 Å resolution. *Acta Crystallogr D Biol Crystallogr* **61**:513-519.

Scott EE, Spatzenegger M, Halpert JR (2001) A truncation of 2B subfamily cytochromes P450 yields increased expression levels, increased solubility, and decreased aggregation while retaining function. *Arch Biochem Biophys* **395**:57-68.

Scott EE, He YA, Wester, MR, White MA, Chin CC, Halpert JR, Johnson EF and Stout CD (2003) An open conformation of mammalian cytochrome P450 2B4 at 1.6 Å resolution. *Proc Natl Acad Sci* USA **100**:13196-13201.

Scott EE, White MA, He YA, Johnson EF, Stout CD and Halpert JR (2004) Structure of mammalian cytochrome P450 2B4 complexed with 4-(4-chlorophenyl)imidazole at 1.9 Å

resolution: insight into the range of P450 conformations and the coordination of redox partner binding. *J Biol Chem* **279**:27294-27301.

Thomas JH (2007) Rapid birth–death evolution specific to xenobiotic cytochrome P450 genes in vertebrates. *PLoS Genetics* **3:**720-728.

Ward BA, Gorski JC, Jones DR, Hall SD, Flockhart DA and Desta Z (2003) The cytochrome P450 2B6 (CYP2B6) is the main catalyst of efavirenz primary and secondary metabolism: implication for HIV/AIDS therapy and utility of efavirenz as a substrate marker of CYP2B6 catalytic activity. *J Pharmacol Exp Ther* **306**:287-300.

Watanabe K, Ohkuri T, Yokobori S and Yamagishi A (2006) Designing thermostable proteins: ancestral mutants of 3-isopropylmalate dehydrogenase designed by using a phylogenetic tree. *J Mol Biol* **355**:664-674.

Xie HJ, Yasar U, Lundgren S, Griskevicius L, Terelius Y, Hassan M and Rane A (2003) Role of polymorphic human CYP2B6 in cyclophosphamide bioactivation. *Pharmacogenomics J* **3**:53-61.

Yano JK, Blasco F, Li H, Schmid RD, Henne A and Poulos TL (2003) Preliminary characterization and crystal structure of a thermostable cytochrome P450 from Thermus thermophilus. *J Biol Chem* **278**:608-616.

Zhao Y, White MA, Muralidhara BK, Sun L, Halpert JR and Stout CD (2006) Structure of microsomal cytochrome P450 2B4 complexed with the antifungal drug bifonazole: insight into P450 conformational plasticity and membrane interaction. *J Biol Chem* **281**:5973-5981.

Zhao YH and Halpert JR (2007) Structure-function analysis of P450 2B. *Biochem Biophys Acta* **1770**: 402-412.

Zanger UM, Klein K, Saussele T, Blievernicht J, Hofmann M and Schwab M (2007) Polymorphic CYP2B6: molecular mechanism and emerging clinical significance, *Pharmacogenomics*, **8** E. Pub. DOI: 10.2217/1462241.6.8.7.

Molecular Pharmacology Fast Forward. Published on August 22, 2007 as DOI: 10.1124/mol.107.039693
This article has not been copyedited and formatted. The final version may differ from this version.

Footnotes to the title

A. This work was supported by National Institutes of Health grant ES03619 and Center Grant ES06676. Yonghong Zhao was supported by NIEHS Training Grant T32 ES07254.

B. Reprint request to:

Santosh Kumar, Ph.D.

Department of Pharmacology and Toxicology

University of Texas Medical Branch

301 University Boulevard

Galveston, TX 77555-1031

Tel: (409) 772-9677

Fax: (409) 772-9642

Email: sakumar@utmb.edu

C. Santosh Kumar and Yonghong Zhao share equal contribution.

Molecular Pharmacology Fast Forward. Published on August 22, 2007 as DOI: 10.1124/mol.107.039693
This article has not been copyedited and formatted. The final version may differ from this version.

Figure legends

Figure 1: Characterization of purified P450 2B6dH. **A.** Absolute spectrum (250-700 nm), **B.** $P450_{reduced}$-CO difference spectrum (400-500 nm).

Figure 2: Homology model of P450 2B6dH based on the crystal structure of P450 2B4 (pdb: 1SUO). The eleven residues picked for rational engineering based on the lower accessibility to bulk solvent are mapped on the structure, and the mutants created are F58L, M103V, V129L, I154V, M198L, L264F, S284H, E350D, Y354H, L390P, and T394S. The molecular graphic was generated using PyMol graphics (DeLano, 2004).

Figure 3: **A.** Thermal inactivation of 2B6dH mutants (1 μM) monitored by a decrease in the amount of P450 as a function of temperature, as described in Materials and Methods. Determination of the total concentration of the heme protein was done by non-linear least square approximation of the spectra by a linear combination of spectral standards of 2B4 low-spin, high-spin and P420-states. The data were fit to a two-state transition to obtain T_m. **B.** Time courses of inactivation of 2B6dH mutants (1 μM) at 45 ^oC monitored as described above. The data were fit to a pseudo-first order equation to obtain k_{inact}.

Figure 4: Characterization of L264F. **A.** Typical type-II difference spectra of 4-CPI binding and **B.** type-I spectra of benzphetamine binding are shown for P450 2B6dH and L264F (left two panels). The binding data with 4-CPI (A) were fit to the tight-binding equation (2B6dH or L264F), while data with benzphetamine (B) were fit to the Michaelis-Menten equation, as

Molecular Pharmacology Fast Forward. Published on August 22, 2007 as DOI: 10.1124/mol.107.039693
This article has not been copyedited and formatted. The final version may differ from this version.

described in Material and Methods, to derive the K_s values as listed in Table 4. **C**. The LC-MS chromatogram of benzphetamine metabolites for the two proteins are shown with the peaks representing a) norbenzphetamine (MW=226.2), b) benzphetamine (240.2), c) OH-norbenzphetamine (242.2) and d) OH-benzphetamine (256.2).

Figure 5: Calorimetric titration profile (*upper panel)* and the resulting integrated binding enthalpy data of 1-BI binding to P450 2B6dH L264F are shown. The data were fit to single-class of binding site model to obtain thermodynamic parameters. *Inset a)* Difference spectra of 1-BI binding and *Inset b)* the thermodynamic signatures (ΔG = open bars, ΔH = filled bars, and -$T\Delta S$= *crossed bars*) of 1-BI binding between P450 2B4dH (Muralidhara et al., 2006) and 2B6dH.

Figure 6: Molecular docking of 1-BI and 4-CPI in the active site of a P450 2B6 homology model. A representative 1-BI and 4-CPI molecules of the lowest energy ensemble (6.17 and 6.52 kcal/mol, respectively) is shown. The point grid used for docking is shown on the heme plane. The mainframe structural loops of the binding pocket are labeled. The molecular graphic was generated using PyMol graphics (DeLano, 2004). Molecular docking was performed using AutoDock Version 3.05 as described earlier (Muralidhara et al., 2006). In brief, the 4-CPI bound P450 2B4dH structure (pdb: 1SUO) was used to model P450 2B6dH using Modeler (http://www.rwmodeler.com/). The R.M.S.D. before and after the minimization using nanoscale molecular dynamics was found to be 0.094 and 0.948, respectively. The homology model was energy minimized and a 40 x 40 x 40-point grid placed at the distal end of the heme was used for 1-BI and 4-CPI docking. A total of 10 unique minimum energy ensembles that exhibited <1 Å

Molecular Pharmacology Fast Forward. Published on August 22, 2007 as DOI: 10.1124/mol.107.039693
This article has not been copyedited and formatted. The final version may differ from this version.

R.M.S.D were ranked, and a representative docking conformation of the lowest energy is presented.

Molecular Pharmacology Fast Forward. Published on August 22, 2007 as DOI: 10.1124/mol.107.039693
This article has not been copyedited and formatted. The final version may differ from this version.

Table 1: Stability of the P450 2B enzymes measured using different methods.

P450	P450 (HS, LS, P420)	Trp-fluorescence	Activity	Heme-dissociation
	T_m (^oC)	$T_{m,app}$ (^oC)	T_{50} (^oC)	$[GuHCl]_{1/2}$ (M)
2B1dH	61.3 ± 0.2[a]	53.9 ± 0.1	52.7 ± 0.3	1.20 ± 0.05
2B4dH	58.9 ± 0.3	52.7 ± 0.3	50.8 ± 0.4	1.26 ± 0.05
2B6dH	48.2 ± 0.2	51.1 ± 0.1	45.2 ± 0.4	0.41 ± 0.02
2B11dH	51.4 ± 0.3	ND	48.4 ± 0.2	ND

[a] Standard errors for fit to the respective equations are shown as ±. Results are representative of at least two independent determinations. The variation between the experiments is ≤10%. ND: Not determined. HS: high spin, LS: low spin

Molecular Pharmacology Fast Forward. Published on August 22, 2007 as DOI: 10.1124/mol.107.039693
This article has not been copyedited and formatted. The final version may differ from this version.

Table 2: Expression of 2B6dH and mutants.

2B6dH	Expression (nmol/L)		
	- Chaperone in TOPP3 cells		+ Chaperone in JM103 cells
	Cell extract	Whole cells	Cell extract
WT	45.3 ± 8.3[a]	ND	152 ± 9.2
F58L	36.6 ± 6.9	ND	nd
M103V	50.1 ± 5.7	ND	nd
V129L	45.5 ± 2.6	ND	141 ± 16[b]
I154V	51.3 ± 21	ND	nd
M198L	154 ± 17	163 ± 16	286 ± 30
L264F	166 ± 32	167 ± 21	306 ± 12
S284H	28.2 ± 12	ND	nd
E350D	70.5 ± 25	ND	nd
Y354H	79.4 ± 13	167 ± 25	210 ± 17
L390P	294 ± 27	367 ± 54	527 ± 29
T394S	69.9 ± 13	ND	nd

[a] Results are the mean ± standard deviation (n = 3). [b] data were obtained as a positive control.

ND: Non-detectible; nd: not determined

Table 3: Stability of P450 2B6dH and mutants measured using different methods.

P450	P450 (HS, LS, and P420)		Trp-fluorescence	Activity	H_2O_2 (60 mM)	Heme-dissociation
	T_m (^oC)	k_{inact} (min^{-1})	$T_{m,app}$ (^oC)	T_{50} (^oC)	k_{inact} (min^{-1})	$[GuHCl]_{½}$ (M)
2B6dH	48.2 ± 0.5[a]	0.034 ± 0.01	51.1 ± 0.1	45.2 ± 0.3	0.025 ± 0.002	0.41 ± 0.02
M198L	46.0 ± 0.4	0.125 ± 0.01	ND	41.5 ± 0.4	0.050 ± 0.003	ND
L264F	52.2 ± 0.5	0.013 ± 0.01	52.6 ± 0.1	46.3 ± 0.2	0.022 ± 0.002	0.56 ± 0.02
L390P	44.2 ± 05	0.157 ± 0.01	51.5 ± 0.2	41.8 ± 0.6	0.042 ± 0.004	0.30 ± 0.03

[a] Standard errors for fit to the respective equations are shown as ±. Results are representative of at least two independent determinations. The variation between the experiments is ≤10%. ND: Not determined; HS: high spin; LS: low spin

Molecular Pharmacology Fast Forward. Published on August 22, 2007 as DOI: 10.1124/mol.107.039693
This article has not been copyedited and formatted. The final version may differ from this version.

Table 4: Binding of pyridine and imidazole derivatives and benzphetamine to P450 2B6dH and L264F.

Ligand	K_s (μM)	
	2B6dH	L264F
4-(4-nitrobenzyl)pyridine (4-NBP)	0.07 ± 0.03[a]	0.05 ± 0.03
4-benzylpyridine (4-BP)	0.53 ± 0.19	0.62 ± 0.20
4-phenylimidazole (4-PI)	0.10 ± 0.04	0.16 ± 0.05
4-(4-chlorophenyl)imidazole (4-CPI)	0.87 ± 0.03	0.98 ± 0.04
1-(2-(benzyloxy)ethyl) imidazole (BEI)	2.06 ± 0.26	2.30 ± 0.92
1-benzylimidazole (1-BI)	2.76 ± 0.14	4.31 ± 1.2
benzphetamine (BP)	52.5 ± 6.5 [b]	61.1 ± 6.6

[a] Standard errors for fit to the respective equations are shown as ±. The high affinity ligands (4-NBP, 4-BP, 4-PI, and 4-CPI) were fit to the tight binding equation, whereas the low affinity ligands (BEI, 1-BI, and BP) were fit to the Hill equation, as described in Materials and Methods. Results are representative of at least two independent determinations. The variation between the experiments is ≤10%. [b] Fit to Michaelis-Menton equation to derive K_s value.

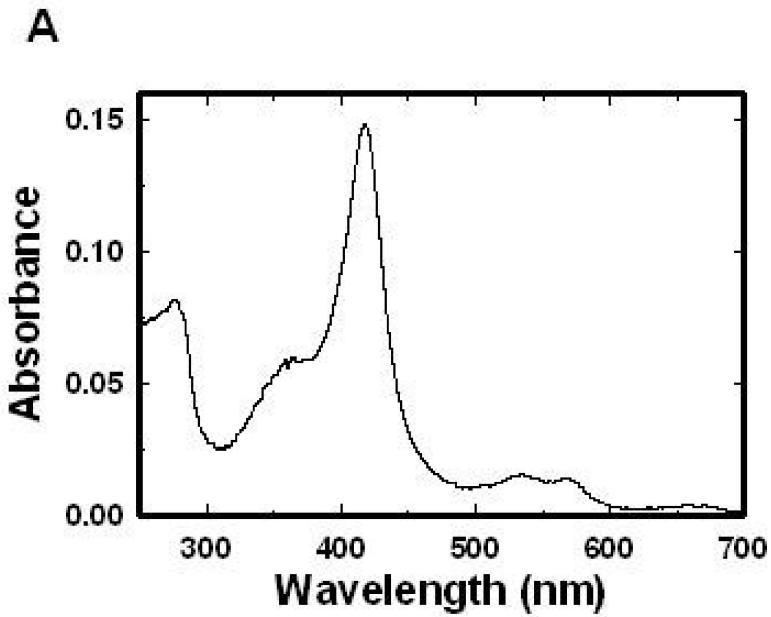

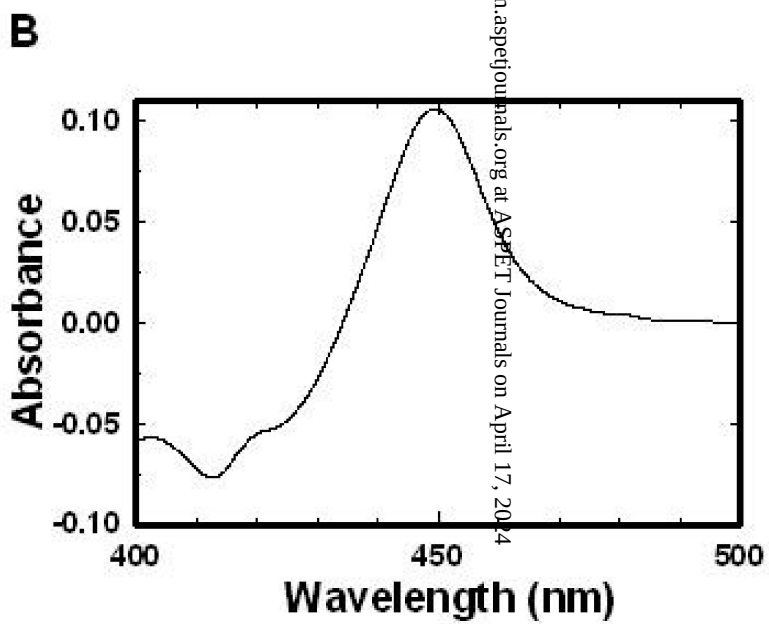

Figure 1

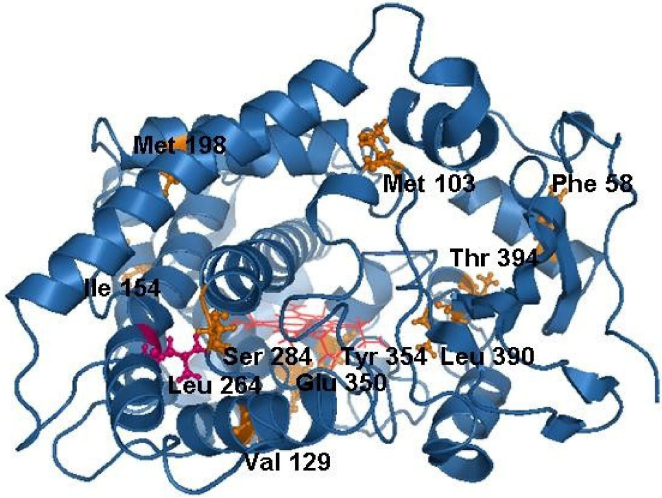
Met 198
Met 103
Phe 58
Thr 394
Ile 154
Ser 284
Tyr 354
Leu 390
Leu 264
Glu 350
Val 129

Figure 2

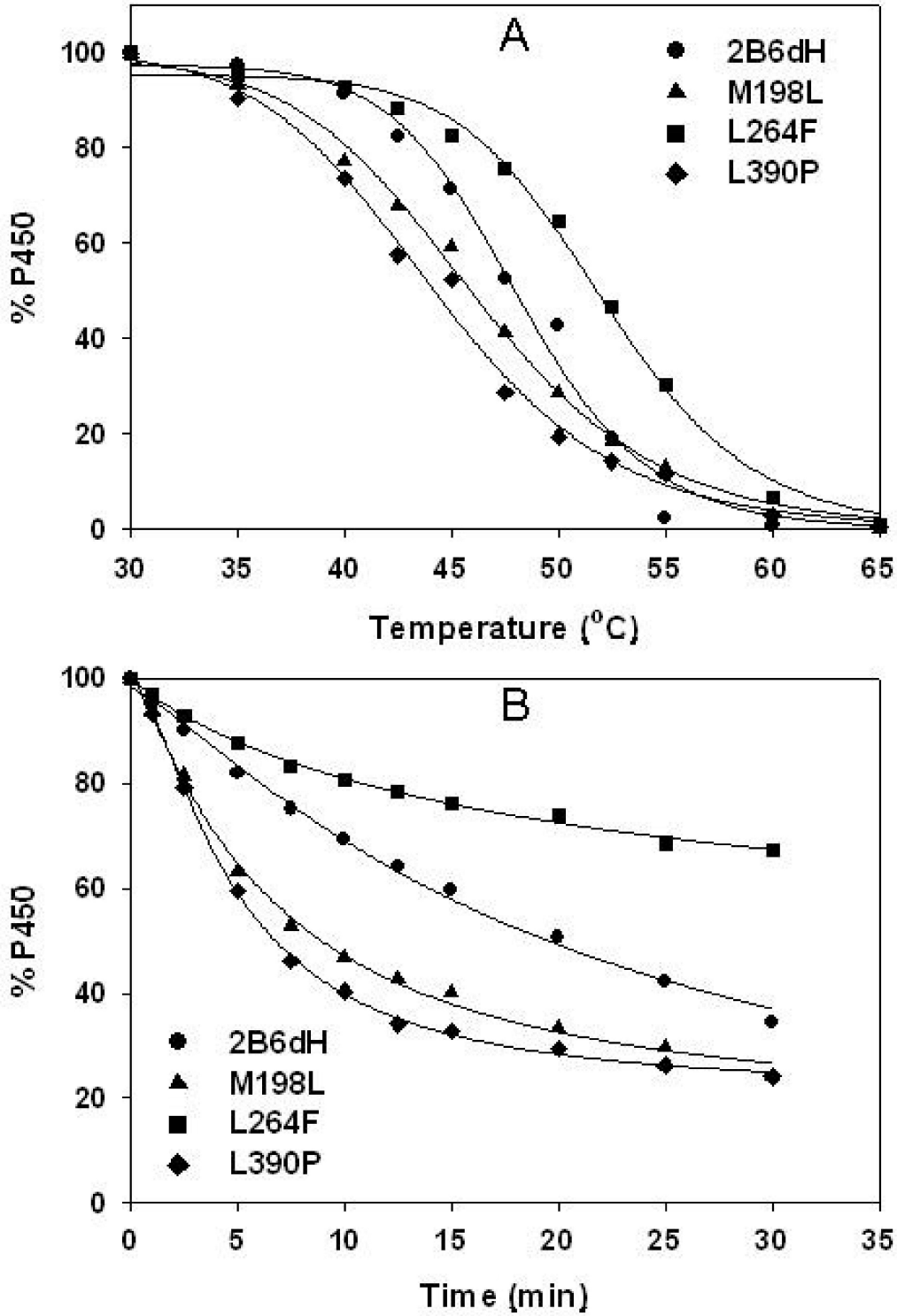

Figure 3

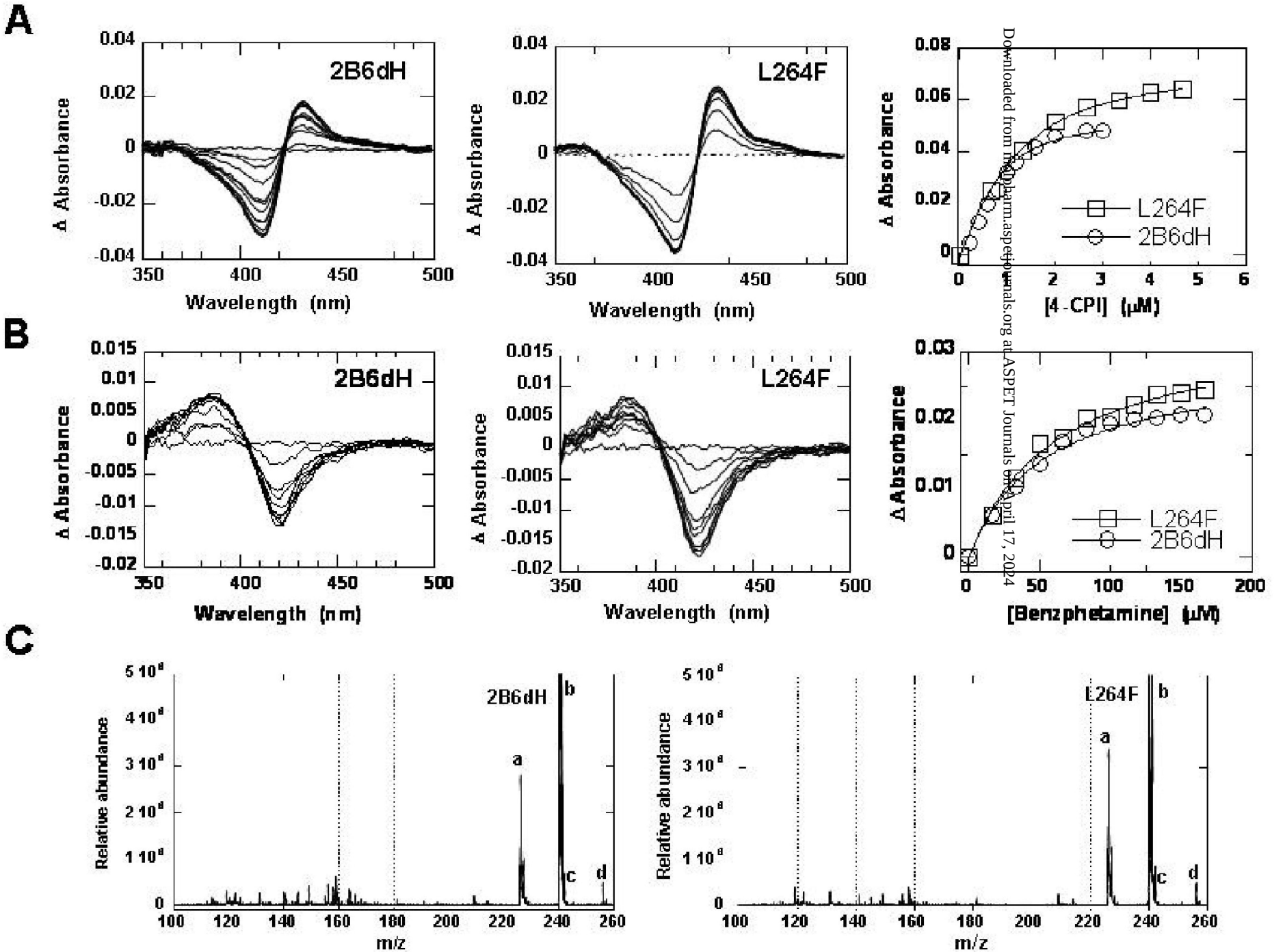

Figure 4

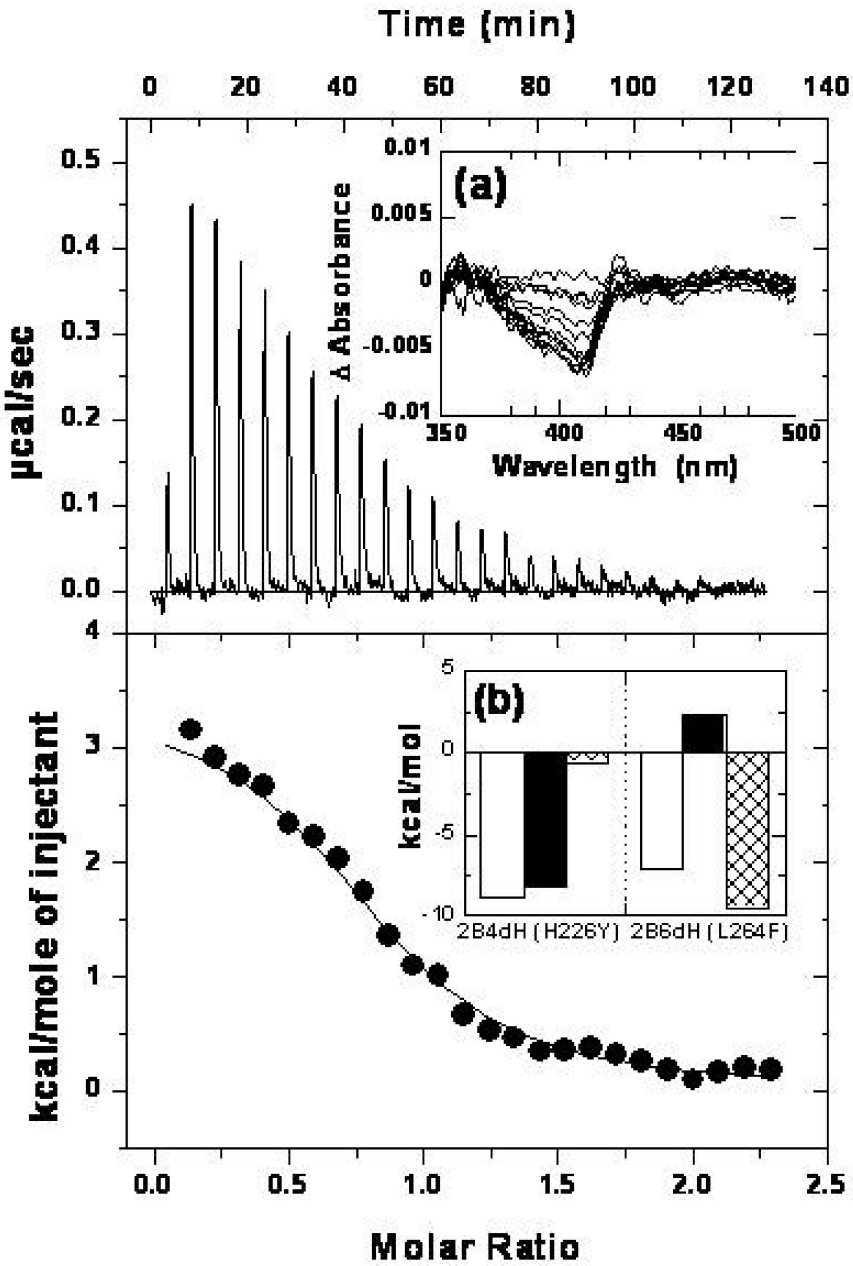

Figure 5

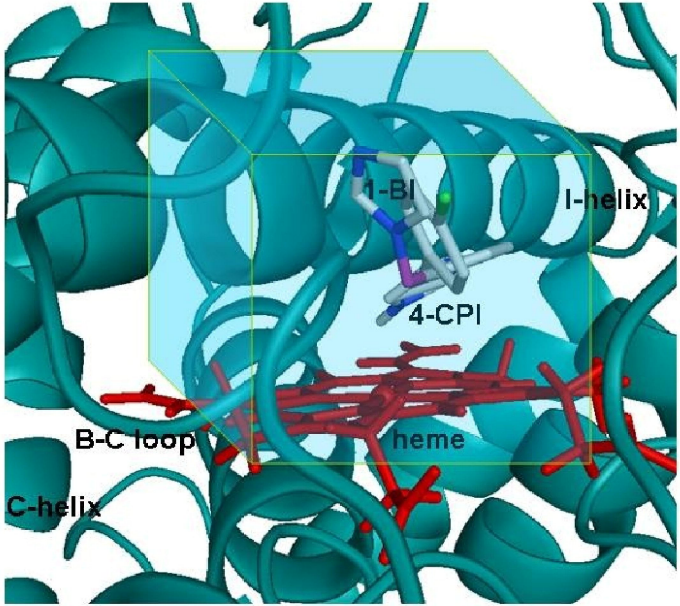

Figure 6